

Stabilization of Metal–Organic Frameworks with High Surface Areas by the Incorporation of Mesocavities with Microwindows

Dan Zhao,[†] Daqiang Yuan,[†] Daofeng Sun,[‡] and Hong-Cai Zhou^{*,†}

Department of Chemistry, Texas A&M University, College Station, Texas 77842, and Department of Chemistry, Shandong University, Jinan 250100, China

Received February 12, 2009; E-mail: zhou@mail.chem.tamu.edu

Ⓜ This paper contains enhanced objects available on the Internet at <http://pubs.acs.org/jacs>.

Metal–organic frameworks (MOFs) are polymers consisting of metal ions/clusters and organic linkers.¹ Because of their porous structures, they may become useful in gas storage, adsorption-based gas/vapor separation, shape/size-selective catalysis, and drug storage and delivery applications and as templates in the preparation of low-dimensional materials.² Their efficacy, especially for applications in gas storage, depends largely on their surface areas. The pore sizes and geometries of MOFs can be tuned at the atomic level, making the discovery of general routes toward MOFs with high surface areas possible.³ Yaghi and co-workers⁴ indicated that exposing the latent edges of phenyl rings within MOFs can lead to significant enhancement of specific surface area, which may serve as a general strategy toward high-surface-area MOFs. Ligand extension is a good way to realize this strategy, as confirmed by calculations on two series of isorecticular MOFs.⁵ However, the discrepancy between the calculated and experimental surface areas became larger as the ligand became more extended, which was attributed to partial collapse of the framework upon guest-molecule removal.^{5a} Most recently, Hupp and co-workers⁶ reported a supercritical processing route to preserve the integrity of the MOFs. Nevertheless, generally as the length of the ligand increases, decreased stability of the ensuing framework or reduced porosity imposed by interpenetration are almost unavoidable.⁷ The solution to this dilemma largely relies on whether the stability and porosity can be reconciled.

Coordination polyhedra are commonly found as either discrete molecules (metal–organic polyhedra) or structural building units within MOFs.⁸ Polyhedron-based MOFs may lead to higher stability and porosity if the sizes of the open windows of the polyhedra are limited. Very common among the polyhedra is the cuboctahedron, which is often constructed with 12 dimetal paddlewheel clusters and 24 isophthalate structural moieties.^{8a–d,f} Connecting the 12 dimetal clusters forms a cuboctahedron, while linking the 24 isophthalate moieties gives rise to a rhombicuboctahedron.^{8r} These polyhedra can be linked to form three-dimensional (3D) MOFs via either coordination bonds or covalent bonds, as demonstrated by Zaworotko and co-workers.^{8l,m,o–r,t} Most recently, a (3,24)-connected network has been reported; it was achieved by connecting the 24 edges of a cuboctahedron (or the 24 corners of a rhombicuboctahedron^{8r}) with a linker having C_3 symmetry.^{8o–q,s} On the basis of this connection mode, an isorecticular series of MOFs can be obtained by changing the size of the linker while keeping the cuboctahedron building units unchanged. If the ligand is extended to nanoscopic range, MOFs containing mesocavities (with one of the dimensions larger than 2 nm) and high surface areas can be obtained. In addition, the sizes of the open windows are controlled

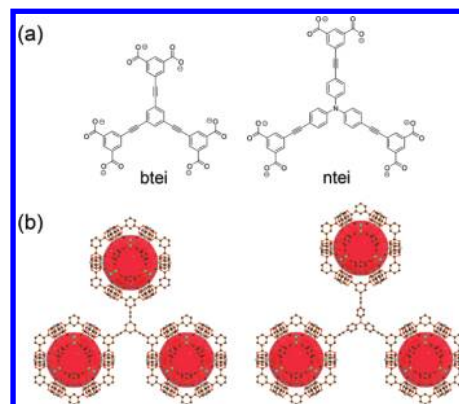


Figure 1. (a) Nanoscopic ligands btei and ntei. (b) Cuboctahedra structural building units in (left) PCN-61 and (right) PCN-66.

by the cuboctahedra and are within the microscopic range (with the largest dimension less than 2 nm), contributing to the stability of the MOF.

Herein we report a strategy for stabilizing MOFs with high surface areas by introducing mesocavities with microwindows into the MOFs based on the (3,24)-connected network. The nanoscopic hexatopic carboxylate ligands designed for this purpose are 5,5',5''-benzene-1,3,5-triyltris(1-ethynyl-2-isophthalate) (btei) and 5,5',5''-(4,4',4''-nitriyltris(benzene-4,1-diyl)tris(ethyne-2,1-diyl))trisiophthalate (ntei) (Figure 1a). Experiments have been designed and performed to answer the following questions: (1) Is the isorecticular series of MOFs based on the (3,24)-connected network achievable? (2) Will the stabilization of MOFs from the limited window sizes offset the destabilization of the MOFs by ligand extension? (3) Will the surface area increase with ligand extension?

Solvothermal reactions of H_6btei and H_6ntei with copper salts yielded two MOFs, $[Cu(H_2O)]_3(btei) \cdot 5DMF \cdot 4H_2O$ (PCN-61) and $[Cu(H_2O)]_3(ntei) \cdot 21DMA \cdot 10H_2O$ (PCN-66), respectively (PCN stands for “porous coordination network”). As expected, PCN-61 and PCN-66 are isostructural (space group $Fm\bar{3}m$); the following discussion of the crystal structure will focus on PCN-61. The three isophthalate moieties in btei are linked through the copper paddlewheel clusters to form the cuboctahedral structural building units, which are covalently linked through the 5-positions of the isophthalate moieties to form a (3,24)-connected network (Figure 1b). The 3D framework can be viewed as the packing of three types of polyhedron: a cuboctahedron, a truncated tetrahedron (T-Td), and a truncated octahedron (T-Oh) (Figure 2). Each truncated triangular face of a T-Td or T-Oh is fully occupied by one ligand. Each cuboctahedron shares its eight triangular faces with eight T-Td’s and its six square faces with six T-Oh’s. The diameters of the colored spheres, which represent the voids inside the three types

[†] Texas A&M University.

[‡] Shandong University.

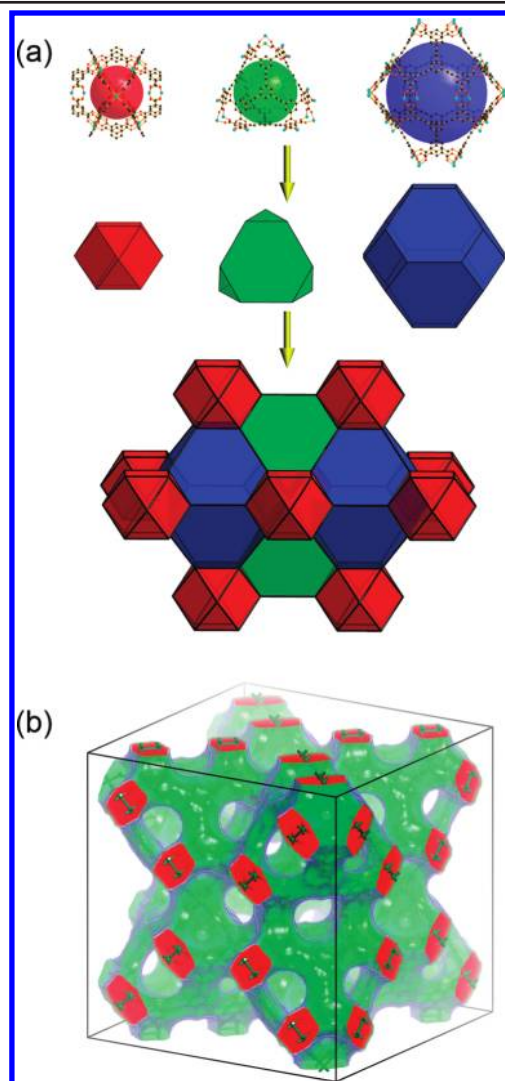


Figure 2. (a) Polyhedra and their 3D packing in PCN-61. (b) Solvent-accessible surface area in PCN-61.

of polyhedra, are 13 Å for the cuboctahedron (red), 15 Å for the T-Td (green), and 23 Å for the T-Oh (blue) (animations illustrating the cuboctahedron, T-Td, and T-Oh and their 3D packing are available). It is evident that increasing the size of the central part of the ligand can further enlarge the size of the T-Oh, which is accompanied by a mild increase in the size of the T-Td and no change in the size of the cuboctahedron. Accordingly, for PCN-66, the diameters are 13 Å for cuboctahedron, 16 Å for the T-Td, and 26 Å for the T-Oh. It is critical that in order to form the aforementioned (3,24)-connected net, the six carboxylate groups in the C_3 -symmetric ligand must be coplanar, although the horizontal mirror plane is not a prerequisite. Both ligands meet this demand, although in the case of nte1, the three phenyl rings around the nitrogen atom are not coplanar.

In both MOFs, crystallinity is retained after the removal of guest molecules, as indicated by the X-ray powder diffraction (XRPD) patterns [Figure S2 in the Supporting Information (SI)]. Such robustness is very rare in MOFs constructed with nanoscopic ligands and confirms our hypothesis that the adoption of cuboctahedra as building units indeed limits the open window size and increases the framework stability. Lah and co-workers^{8q} reported a similar (3,24)-connected MOF based on zinc paddlewheel clusters. However, their MOF was not stable upon the removal of guest molecules, probably because of (1) the nonrigid ligand they adopted

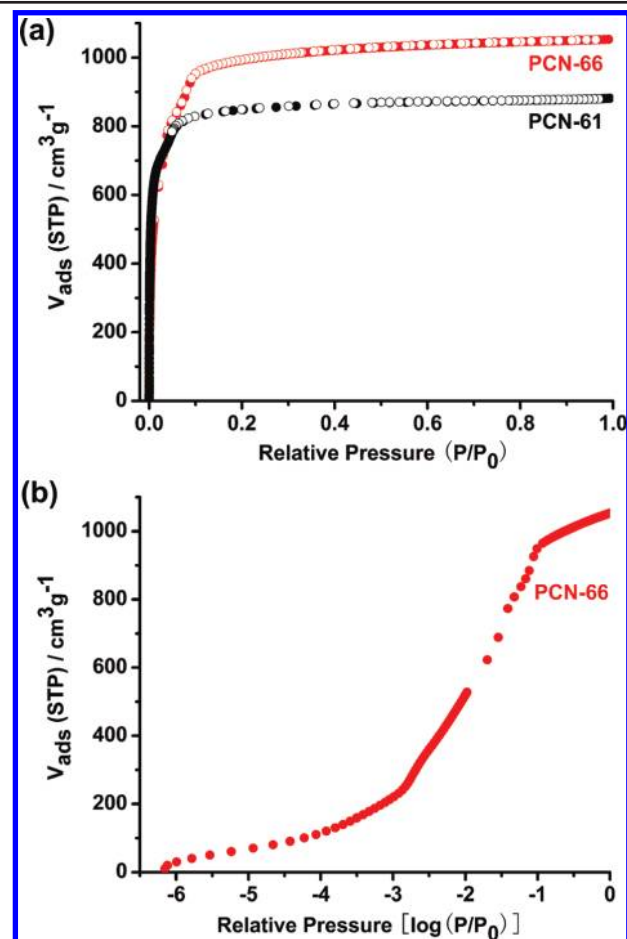


Figure 3. (a) N_2 sorption isotherms for PCN-61 (black) and PCN-66 (red) at 77 K (●, adsorption; ○, desorption). (b) Amount of nitrogen adsorbed in PCN-66 at 77 K vs $\log(P/P_0)$.

and (2) the instability of the zinc paddlewheel clusters after axial ligand removal during activation. PCN-60, the zinc paddlewheel counterpart of PCN-61, was synthesized and fully characterized (see the SI), and it also suffers from this instability during activation. Even when treated with the mild supercritical drying process, PCN-60 still exhibited a very low nitrogen adsorption capacity.⁶ The scanning electron microscopy (SEM) images in Figure S3 show that in as-synthesized and the activated PCN-61, the crystals had the same ordered shape. In PCN-60, however, the crystals shrank upon the removal of guest molecules, indicating framework disintegration. This instability was further confirmed by XRPD patterns (Figure S2). In conclusion, in order to stabilize the (3,24)-connected MOFs, rigid ligands and stable paddlewheel clusters (such as dicopper and dinickel) should be adopted. Our speculation is supported by a recently published stable (3,24)-connected MOF in which a rigid ligand and the dicopper paddlewheel cluster were adopted.^{8s}

From the foregoing discussion of the crystal structure, it is evident that the sizes of the cavities within the two MOFs range from microporous (cuboctahedron and T-Td) to mesoporous (T-Oh). This hierarchical porous structure is reflected in the N_2 sorption isotherms collected at 77 K (Figure 3a). The hybrid porous structures exhibit reversible pseudo-type-I isotherms with a small step before the plateau appears, as is typical in MOFs with both micro- and mesopores.^{8o,p,s,9} We believe that this is due to the occurrence of multilayer sorption in the larger cavities after the formation of a single layer at low pressure. This is confirmed by the three distinct sorption regions within PCN-66, corresponding to the three

Table 1. Surface Areas, Pore Volumes, and Porosities of Selected MOFs

material	surface area (m ² g ⁻¹) (Langmuir/BET/calcd ^a)	pore volume (cm ³ g ⁻¹) (exptl/calcd ^a)	porosity (%) ^a
MOF-5 ^b	4400/3800/3110	1.04/1.31	77.9
IRMOF-20 ^c	4593/4024/3125	1.53/1.58	80.9
MOF-177 ^d	5640/4746/3654	1.59/1.87	80.0
MIL-101 ^e	5900/4100/3252	2.00/1.95	82.0
PCN-61	3500/3000/3455	1.36/1.37	77.0
PCN-66	4600/4000/3935	1.63/1.75	78.1

^a Calculated using Material Studio 4.4. ^b Data from refs 1a and 11. ^c Data from ref 12. ^d Data from refs 4 and 12a. ^e Data from ref 9a.

different-sized cavities discussed above (Figure 3b). Although its validity in microporous materials has been questioned, the Brunauer–Emmett–Teller (BET) method is still widely used to estimate the surface areas of MOFs.¹⁰ The two criteria discussed in the literature have been strictly followed to decide the pressure range for applying the BET analysis.^{5a} With the BET model, an activated PCN-61 sample was estimated to have a specific surface area of 3000 m² g⁻¹, and the Langmuir surface area was 3500 m² g⁻¹ assuming monolayer coverage. For PCN-66, where the larger ligand was used, there was a remarkable increase in surface area (BET, 4000 m² g⁻¹; Langmuir, 4600 m² g⁻¹), which supports our hypothesis that the expansion of the ligand leads to increased surface area. To the best of our knowledge, PCN-66 possesses the highest surface area reported to date for MOFs based on paddlewheel clusters, and it is also among the highest reported (Table 1). It can be extrapolated that use of even larger hexatopic carboxylate ligands may lead to stable MOFs with even higher surface areas.

In conclusion, two isorecticular MOFs built using nanoscopic ligands and having (3,24)-connected networks containing mesocavities with microwindows were synthesized. The stabilities of these MOFs were increased by the in situ formation of coordination cuboctahedra building units, which limit the open window sizes of the mesocavities. The surface area of the activated MOF was increased remarkably by ligand extension, presumably as a result of the increased size of the mesocavities. The combination of the (3,24)-connected network topology with the larger ligand demonstrated that the incorporation of mesocavities with microwindows may serve as a general approach toward stable MOFs with higher surface areas. Work along this line is currently underway in our laboratory and will be reported soon.

Acknowledgment. This work was supported by the U.S. Department of Energy (DE-FC36-07GO17033), the U.S. Defense Logistics Agency (N00164-07-P-1300), and the U.S. National Science Foundation (CHE-0449634). The microcrystal diffraction was carried out at the Advanced Photon Source on beamline 15ID-C with the kind assistance of Yu-Sheng Chen at Argonne National Laboratory (CHE-0535644, DEAC02-06CH11357). We acknowledge Dr. Shuisong Ni, Dr. Shengqian Ma, and Dr. Xi-Sen Wang for their help with the X-ray crystallography and gas-sorption measurements.

Supporting Information Available: Crystallographic data for PCN-60, -61, and -66 (CIF), experimental details, thermogravimetric analysis

curves, XRPD patterns, SEM images, figures for PCN-66, and complete ref 9c. This material is available free of charge via the Internet at <http://pubs.acs.org>.

References

- (1) (a) Li, H. L.; Eddaoudi, M.; O'Keeffe, M.; Yaghi, O. M. *Nature* **1999**, *402*, 276. (b) Kitagawa, S.; Kitaura, R.; Noro, S. *Angew. Chem., Int. Ed.* **2004**, *43*, 2334. (c) Férey, G. *Chem. Soc. Rev.* **2008**, *37*, 191. (d) Robson, R. *Dalton Trans.* **2008**, 5113.
- (2) (a) Rosi, N. L.; Eckert, J.; Eddaoudi, M.; Vodak, D. T.; Kim, J.; O'Keeffe, M.; Yaghi, O. M. *Science* **2003**, *300*, 1127. (b) Zhao, D.; Yuan, D. Q.; Zhou, H. C. *Energy Environ. Sci.* **2008**, *1*, 222. (c) Eddaoudi, M.; Kim, J.; Rosi, N.; Vodak, D.; Wachter, J.; O'Keeffe, M.; Yaghi, O. M. *Science* **2002**, *295*, 469. (d) Ma, S. Q.; Sun, D. F.; Simmons, J. M.; Collier, C. D.; Yuan, D. Q.; Zhou, H. C. *J. Am. Chem. Soc.* **2008**, *130*, 1012. (e) Ma, S. Q.; Sun, D. F.; Wang, X. S.; Zhou, H. C. *Angew. Chem., Int. Ed.* **2007**, *46*, 2458. (f) Horike, S.; Dincă, M.; Tamaki, K.; Long, J. R. *J. Am. Chem. Soc.* **2008**, *130*, 5854. (g) Alkordi, M. H.; Liu, Y. L.; Larsen, R. W.; Eubank, J. F.; Eddaoudi, M. *J. Am. Chem. Soc.* **2008**, *130*, 12639. (h) Horcajada, P.; Serre, C.; Vallet-Regí, M.; Sebban, M.; Taulerelle, F.; Férey, G. *Angew. Chem., Int. Ed.* **2006**, *45*, 5974. (i) Liu, B.; Shioyama, H.; Akita, T.; Xu, Q. *J. Am. Chem. Soc.* **2008**, *130*, 5390.
- (3) (a) Férey, G. *J. Solid State Chem.* **2000**, *152*, 37. (b) Mellot-Draznieks, C.; Dutour, J.; Férey, G. *Angew. Chem., Int. Ed.* **2004**, *43*, 6290. (c) Férey, G.; Mellot-Draznieks, C.; Serre, C.; Millange, F. *Acc. Chem. Res.* **2005**, *38*, 217. (d) Eddaoudi, M.; Moler, D. B.; Li, H. L.; Chen, B. L.; Reineke, T. M.; O'Keeffe, M.; Yaghi, O. M. *Acc. Chem. Res.* **2001**, *34*, 319. (e) Yaghi, O. M.; O'Keeffe, M.; Ockwig, N. W.; Chae, H. K.; Eddaoudi, M.; Kim, J. *Nature* **2003**, *423*, 705.
- (4) Chae, H. K.; Siberio-Pérez, D. Y.; Kim, J.; Go, Y. B.; Eddaoudi, M.; Matzger, A. J.; O'Keeffe, M.; Yaghi, O. M. *Nature* **2004**, *427*, 523.
- (5) (a) Walton, K. S.; Snurr, R. Q. *J. Am. Chem. Soc.* **2007**, *129*, 8552. (b) Han, S. S.; Goddard, W. A. *J. Phys. Chem. C* **2008**, *112*, 13431.
- (6) Nelson, A. P.; Farha, O. K.; Mulfort, K. L.; Hupp, J. T. *J. Am. Chem. Soc.* **2009**, *131*, 458.
- (7) (a) Wang, X. S.; Ma, S. Q.; Sun, D. F.; Parkin, S.; Zhou, H. C. *J. Am. Chem. Soc.* **2006**, *128*, 16474. (b) Ma, S. Q.; Sun, D. F.; Ambrogio, M.; Fillinger, J. A.; Parkin, S.; Zhou, H. C. *J. Am. Chem. Soc.* **2007**, *129*, 1858.
- (8) (a) Eddaoudi, M.; Kim, J.; Wachter, J. B.; Chae, H. K.; O'Keeffe, M.; Yaghi, O. M. *J. Am. Chem. Soc.* **2001**, *123*, 4368. (b) Abourahma, H.; Coleman, A. W.; Moulton, B.; Rather, B.; Shahgaldian, P.; Zaworotko, M. J. *Chem. Commun.* **2001**, 2380. (c) Moulton, B.; Lu, J. J.; Mondal, A.; Zaworotko, M. J. *Chem. Commun.* **2001**, 863. (d) Ke, Y. X.; Collins, D. J.; Zhou, H. C. *Inorg. Chem.* **2005**, *44*, 4154. (e) Ni, Z.; Yassar, A.; Antoun, T.; Yaghi, O. M. *J. Am. Chem. Soc.* **2005**, *127*, 12752. (f) Furukawa, H.; Kim, J.; Plass, K. E.; Yaghi, O. M. *J. Am. Chem. Soc.* **2006**, *128*, 8398. (g) Moulton, B.; Zaworotko, M. J. *Chem. Rev.* **2001**, *101*, 1629. (h) Seidel, S. R.; Stang, P. J. *Acc. Chem. Res.* **2002**, *35*, 972. (i) Fujita, M.; Tominaga, M.; Hori, A.; Therrien, B. *Acc. Chem. Res.* **2005**, *38*, 371. (j) Tranchemontagne, D. J.; Ni, Z.; O'Keeffe, M.; Yaghi, O. M. *Angew. Chem., Int. Ed.* **2008**, *47*, 5136. (k) Lu, J. J.; Mondal, A.; Moulton, B.; Zaworotko, M. J. *Angew. Chem., Int. Ed.* **2001**, *40*, 2113. (l) McManus, G. J.; Wang, Z. Q.; Zaworotko, M. J. *Cryst. Growth Des.* **2004**, *4*, 11. (m) Perry, J. J.; Kravtsov, V. C.; McManus, G. J.; Zaworotko, M. J. *J. Am. Chem. Soc.* **2007**, *129*, 10076. (n) Cairns, A. J.; Perman, J. A.; Wojtas, L.; Kravtsov, V. C.; Alkordi, M. H.; Eddaoudi, M.; Zaworotko, M. J. *J. Am. Chem. Soc.* **2008**, *130*, 1560. (o) Nouar, F.; Eubank, J. F.; Bousquet, T.; Wojtas, L.; Zaworotko, M. J.; Eddaoudi, M. *J. Am. Chem. Soc.* **2008**, *130*, 1833. (p) Chun, H. *J. Am. Chem. Soc.* **2008**, *130*, 800. (q) Zou, Y.; Park, M.; Hong, S.; Lah, M. S. *Chem. Commun.* **2008**, 2340. (r) Wang, X. S.; Ma, S. Q.; Forster, P. M.; Yuan, D. Q.; Eckert, J.; López, J. J.; Murphy, B. J.; Parise, J. B.; Zhou, H. C. *Angew. Chem., Int. Ed.* **2008**, *47*, 7263. (s) Yan, Y.; Lin, X.; Yang, S. H.; Blake, A. J.; Dailly, A.; Champness, N. R.; Hubberstey, P.; Schröder, M. *Chem. Commun.* **2009**, 1025. (t) Perry, J. J.; Perman, J. A.; Zaworotko, M. J. *Chem. Soc. Rev.* **2009**, *38*, 1400.
- (9) (a) Férey, G.; Mellot-Draznieks, C.; Serre, C.; Millange, F.; Dutour, J.; Surlé, S.; Margiolaki, I. *Science* **2005**, *309*, 2040. (b) Fang, Q. R.; Zhu, G. S.; Jin, Z.; Ji, Y. Y.; Ye, J. W.; Xue, M.; Yang, H.; Wang, Y.; Qiu, S. L. *Angew. Chem., Int. Ed.* **2007**, *46*, 6638. (c) Park, Y. K. *Angew. Chem., Int. Ed.* **2007**, *46*, 8230. (d) Koh, K.; Wong-Foy, A. G.; Matzger, A. J. *Angew. Chem., Int. Ed.* **2008**, *47*, 677.
- (10) Brunauer, S.; Emmett, P. H.; Teller, E. *J. Am. Chem. Soc.* **1938**, *60*, 309.
- (11) Kaye, S. S.; Dailly, A.; Yaghi, O. M.; Long, J. R. *J. Am. Chem. Soc.* **2007**, *129*, 14176.
- (12) (a) Wong-Foy, A. G.; Matzger, A. J.; Yaghi, O. M. *J. Am. Chem. Soc.* **2006**, *128*, 3494. (b) Rowsell, J. L. C.; Yaghi, O. M. *J. Am. Chem. Soc.* **2006**, *128*, 1304.

JA901109T